R-1718-PR
February 1975

Far Infrared and Submillimeter Scattering II. Attenuation by Clouds and Rain

D. Deirmendjian

A Report prepared for

UNITED STATES AIR FORCE PROJECT RAND

Rand
SANTA MONICA, CA. 90406

R-1718-PR
February 1975

Far Infrared and Submillimeter Scattering II. Attenuation by Clouds and Rain

D. Deirmendjian

A Report prepared for

UNITED STATES AIR FORCE PROJECT RAND

Rand
SANTA MONICA, CA. 90406

Published by The Rand Corporation

PREFACE

This is the second and final part of a study designed to assist the Air Force in the choice of possible new target acquisition and communication systems in the far infrared and submillimeter region of the electromagnetic spectrum. It provides reliable estimates of the attenuation of radiation at such wavelengths through various types of water clouds as well as moderate and heavy rain.

The work leading to the reported results was supported within Air Force Project RAND. The presentation here was completed partly with the author's own support. It should be useful to analysts in DCS/Research and Development at Hq USAF, the Air Force Systems Command, and other DoD agencies concerned with the far infrared and submillimeter scattering properties of clouds and rain.

Related Rand studies include R-456-PR, *Electromagnetic Scattering on Spherical Polydispersions* (D. Deirmendjian, 1969); R-1486-PR, *Far Infrared and Submillimeter Scattering I. The Optical Constants of Water--A Survey* (D. Deirmendjian, 1974); and R-1335-ARPA, *Atmospheric Effects on Terrestrial Millimeter-Wave Communications* (J. S. Dudzinsky, 1974).

SUMMARY

In this second part of our study on far infrared and submillimeter atmospheric scattering effects, we use the optical constants surveyed in the first part [Deirmendjian, 1974] to estimate extinction coefficients over the wavelength range between $\lambda 12$ μm and $\lambda 2$ cm. For this purpose we set up new analytic drop-size distribution models to simulate fog, precipitating clouds, and rain corresponding to rainfall rates of 10 and 50 mm hr^{-1}.

The results, in the form of volume extinction and absorption coefficients computed according to polydisperse Mie scattering theory at specific wavelengths, are presented in tables and graphically in plots allowing for accurate interpolation for any desired wavelength within the range.

It is found that cloud extinction, of the order of 50 nepers or 200 decibels per kilometer, may exceed rain extinction by large factors for $\lambda \lesssim 100$ μm waves, whereas for wavelengths longer than $\lambda 200$ μm, under near-saturated conditions, water vapor absorption should be the dominant attenuator. The greatest attenuation by heavy rain may be expected around $\lambda 5$ mm with a value of about 5 nepers or 20 decibels per kilometer. These theoretical estimates compare well with available observation and other authors' approximations.

Our results imply that the interference with current tactical air operations by clouds and fog can be substantially reduced if target acquisition and munitions guidance systems that operate at frequencies near 230 GHz can be developed.

ACKNOWLEDGMENTS

The kind assistance of the late Dr. John Chamberlain of the National Physical Laboratory, Teddington, England, in making freely available upon request his prepublication laboratory results is gratefully acknowledged. The author is primarily indebted to R. Robert Rapp for his encouragement and moral support to undertake and complete this study. The assistance of C. C. Chen and R. R. Rapp in reading the original manuscript is also acknowledged.

CONTENTS

PREFACE iii

SUMMARY v

ACKNOWLEDGMENTS vii

Section

1. INTRODUCTION 1

2. EXTINCTION COEFFICIENT FOR POLYDISPERSIONS 3

3. DROP-SIZE DISTRIBUTION FUNCTIONS 7

4. CHOICE OF WAVELENGTHS AND OPTICAL CONSTANTS 13

5. EXTINCTION COEFFICIENTS FOR CLOUDS AND RAIN 17

6. DISCUSSION AND CONCLUSIONS 25

REFERENCES 31

1. INTRODUCTION

In the first part of this study [Deirmendjian, 1974], which was devoted to a survey of the optical constants of water, we outlined the reasons why we believed it to be both desirable and feasible to obtain some reliable estimates of the far infrared and submillimeter scattering properties of clouds and rain. In particular, we mentioned the development of new sources of coherent electromagnetic waves in this part of the spectrum. As a matter of fact, from a more recent special conference, it was evident that these new sources are being developed at an accelerated rate and that they will cover the spectrum with a high degree of resolution [Button, 1974].

There is no doubt that these new sources will find many scientific and technical applications. Some of these will inevitably be concerned with the terrestrial atmosphere either as a subject of direct study, for example through spectroscopy, or indirectly as a disturbance interposed between source and receiver. One kind of disturbance, namely the simplest type of electromagnetic scattering, is connected to both aspects: as a diagnostic of particulates through the study of the directional variation of scattered intensity and its polarization, and as an attenuating disturbance through the absorption and scattering cross section of the particles. As is well known, the most efficient scattering is produced by particles whose linear dimensions are of the order of the wavelength of the incident radiation. Hence our concern with cloud and rain particles, whose diameters of tens and hundreds of micrometers are just right for maximum interaction with *far infrared* ($15 \lesssim \lambda \lesssim 100$ μm) and *submillimeter* ($100 \lesssim \lambda \lesssim 1000$ μm) waves.

In the present report we shall concentrate mainly on the attenuation (or extinction) properties of the hydrometeors, leaving the directional scattering properties for a separate study. In particular, we first briefly describe and justify the use of some new cloud- and raindrop-size distribution models that we developed expressly for this study. We then present the results of attenuation computations for these models using selected optical constants from data summarized in

Part I [Deirmendjian, 1974] and polydisperse scattering theory and its application as developed earlier [Deirmendjian, 1969]. Finally we analyze and compare our estimates with other work and with observation, where possible, and discuss their implications in atmospheric applications.

2. EXTINCTION COEFFICIENT FOR POLYDISPERSIONS

Let us briefly outline the theory of polydisperse scattering to be used. Assume that the number density in a typical volume of air containing cloud or rain droplets may be described by a continuous function n(r), where r is the radius of the spherical particles. Then, if $\sigma_{ex}(m,r)$ is the extinction (scattering + absorption) cross section as a function of r and the optical constants ν and κ, where $m \equiv \nu - i\kappa$ is the complex index of refraction, it can be shown that

$$\beta_{ex}[\lambda,m,n(r)] = \int_{r_1}^{r_2} \sigma_{ex}(m,r)n(r)dr \qquad (1)$$

is the *volume extinction coefficient* for the polydispersion, r_1 and r_2 are the lower and upper limits in the droplet size, and λ is the wavelength of the incident radiation. The latter may be a narrow band of incoherent radiation or a coherent, monochromatic wave train, provided that the distance between drops is large with respect to λ and that their distribution is random and nonstationary.

It is well known that, for spherical particles of finite size with respect to λ, the behavior of σ_{ex} is highly dependent on r and m, as pointed out by many authors, particularly van de Hulst [1957], who also discusses various special cases and approximations. In the present case, we shall use the exact theory, where the extinction efficiency, or normalized cross section $K_{ex}(m,x) \equiv \sigma_{ex}/(\pi r^2)$ is given by the corresponding Mie series. As is well known, the terms in this series contain ratios of Ricatti-Bessel functions of real or complex argument involving the normalized size $x = 2\pi r/\lambda$ and m, and they can be computed using appropriate programs for high-speed data processing systems [see, e.g., Deirmendjian, 1969].

For a polydispersion, the extinction integral in (1), after a change of variable and using the nondimensional form of the extinction, may be rewritten in the form [Deirmendjian, 1969]

$$\beta_{ex}(\lambda,m,n) = \pi\left(\frac{\lambda}{2\pi}\right)^3 \int_{x_1}^{x_2} x^2 n(x) K_{ex}(m,x)\,dx \qquad (2)$$

where $n(x)dx = (\lambda/2\pi)n(r)dr$. From the foregoing, it is clear that for polydispersions containing mainly finite-sized particles with respect to the wavelength, β_{ex} is critically dependent on the form and magnitude of $n(x)$, the size range of the particles, as well as on their optical constants.

For other conditions, two limiting cases are worth recalling: the geometric optics or large sphere approximation with $\lambda << r$; and the long wave (low frequency) or small particle approximation, with $r << \lambda$, where the shape of the particle is unimportant. In the first case, provided the spheres are lossy and $\kappa \neq 0$, it is well known by physical argument [van de Hulst, 1957] and mathematical treatment of the Mie series [Chýlek, 1973] that the $x \to \infty$ limit of K_{ex} is 2. Hence if *all* the particles in the polydispersion are in the geometric optics domain, we have from (1)

$$\beta_{ex}[n(r)] = 2\pi \int_{r_1}^{r_2} r^2 n(r)\,dr, \quad \lambda << r; \quad \kappa \neq 0 \qquad (3)$$

or twice the sum of the geometrical cross-sectional areas of all the particles in a unit volume. Clearly the value of β_{ex} in this case is independent of the wavelength and the optical constants but very much a function of the density distribution $n(r)$.

In the case of large, nonabsorbing spheres, where $\kappa = 0$, the $x \to \infty$ limit of the scattering or extinction cross section does not exist, as conjectured by Deirmendjian [1969] and rigorously demonstrated by Chýlek [1973]. However the Mie series values for large x do show increasingly "rapid" oscillations around 2 as x increases, so that in this case also the integration (3) may be a good approximation for continuous and smooth size distribution functions. At any rate this question is not of concern here, since we are dealing with the infrared spectrum where liquid water always shows some absorption.

In the other limit, a small particle approximation for the extinction may be given as a power series in the size parameter x [van de Hulst, 1957; Penndorf, 1962]. In particular, it can be shown by comparison with the exact Mie values [Deirmendjian, 1963] that the first term in x in such a series, that is

$$K_{ex}(m,x) = \frac{24\nu\kappa}{Z}\, x, \qquad x << 1 \tag{4}$$

with

$$Z \equiv (\nu^2+\kappa^2)^2 + 4(\nu^2-\kappa^2+1)$$

may be sufficient, provided κ is not small compared to 1 and $x \lesssim 0.01$. Expression (4) represents also the normalized absorption cross section K_{ab} in the Rayleigh approximation, in which case $K_{ab} \to K_{ex}$, $K_{sc} \to 0$ for any value of κ no matter how small, provided x is sufficiently small [Deirmendjian, 1969]. The extinction cross section itself may be obtained from (4) in terms of the volume v occupied by the particle, after multiplying both sides of (4) by πr^2 and replacing x, that is

$$\pi r^2 K_{ex} = \sigma_{ex} = \frac{36\pi\nu\kappa}{Z}\,\frac{v}{\lambda} \quad . \tag{5}$$

The extension of this result to a polydispersion follows easily by substituting (5) into (1) to obtain

$$\beta_{ex} = \beta_{ab} = \frac{36\pi\nu\kappa}{Z}\,\frac{1}{\lambda}\, V_p, \qquad r_2 << \lambda \tag{6}$$

where

$$V_p \equiv \frac{4}{3}\,\pi \int_{r_1}^{r_2} r^3 n(r)\,dr \tag{7}$$

is the volume of all the particles in the polydispersion per unit volume of space. It is noted that (6) is strictly valid only when the

largest particle r_2 is itself much smaller than λ, but this restriction may be relaxed depending on the nature of the density function n(r).

From (6) and (7) it is also clear that in this limiting case the form of the density function does not affect the extinction if the volume mixing ratio V_p remains constant.

3. DROP-SIZE DISTRIBUTION FUNCTIONS

For the size distribution function we shall use the general form

$$n(r) = a\, r^{\alpha} \exp\,(-br^{\gamma}) \tag{8}$$

first used by this author [Deirmendjian, 1962] to model both clouds and hazes, as well as raindrops [Deirmendjian, 1963]. This function vanishes for very small and large sizes and has a single maximum. The constants a, α, b, and γ are real positive numbers that may be related to measurable parameters. For example, for the special case $\gamma = 1$, it can be easily shown by integration of (8) with respect to the radius r between r = 0 and ∞ that

$$a = N\,\frac{b^{\alpha+1}}{\Gamma(\alpha+1)} \tag{9}$$

where N is the total number of particles per unit volume in the distribution. Similarly the constant b is given by the mode radius r_c or size of greatest frequency by means of the relation $b = \alpha/r_c$.

We note in passing that recently Hansen [1971] has introduced a distribution function which is identical to (8), except for a redefinition of the constants in terms of other quantities, without additional physical justification in our opinion. The conversion from one set of constants to the other is easily derived by comparing the two forms.

Among the desirable properties of the form (8) is the exponential decay in number density with increasing drop size. This and the nature of the Mie functions result in a rapid convergence of the integrals of type (2) under the condition

$$r_2 > \frac{\alpha+4}{b}\,, \qquad \gamma = 1 \tag{10}$$

where r_2 is the radius corresponding to the upper limit x_2 of integration. This behavior closely corresponds to natural atmospheric

polydispersions where there is a cutoff of the distribution at the upper end due to various processes.

At the lower end the density function (8) also vanishes, due to the power factor, again corresponding to natural conditions. Thus the integral (2) may be replaced by a definite one between the limits $0 \leqq r \leqq \infty$ without loss of applicability.

Among the several models of the type (8) introduced earlier to simulate various atmospheric particles [Deirmendjian, 1962, 1963, 1969] our haze H, L, M models and cloud C.1 model for fair weather cumulus have been found particularly useful in various applications of radiative transfer theory to problems related to the atmospheres of the earth and Venus [see, e.g., Hansen, 1971; Thompson and Wells, 1971; Kattawar and Plass, 1975]. The prevalent drop sizes in the cloud C.1 model, however, are too small and their range too narrow to simulate precipitating type clouds. For the present work we shall introduce two new cloud density functions to simulate precipitating stratus or nimbostratus, called *cloud C.5*, and a large droplet component, called *cloud C.6*. These choices have been suggested by measurements, such as Okita's [1961], and others, taken within clouds that are producing precipitation. Further justification for their choice and other details will be discussed in a projected future study.

The specific forms of our new density functions are as follows. For cloud C.5, we have

$$n(r) = a\, r^4\, e^{-2r/3}\ \mathrm{cm}^{-3}\ \mu\mathrm{m}^{-1} \tag{11}$$

where $r_c = 6\ \mu$m, and the constant a is to be determined by N according to (9). For a nominal density of 100 droplets per cm^3, this model shows a liquid water content of 0.297 g m^{-3}.*

For cloud C.6 we adopted the formula

---

*It is interesting to note that Hansen's [1971] "mean effective radius" and "effective variance" corresponding to our C.5 distribution (10.5 μm and 0.143, respectively) coincide almost exactly with those of Diem's measured distributions for cumulus congestus and nimbostratus clouds as reduced by Hansen [1971].

$$n(r) = a\, r^2\, e^{-r}\ \text{cm}^{-3}\ \mu\text{m}^{-1} \qquad (12)$$

where r_c = 20 μm. For a typical density of 10^{-1} drop per cm^3, this component is equivalent to a water content of 0.025 g m^{-3}. We note that a linear combination of the density functions (11) and (12) reproduces some of Okita's [1961] measured droplet spectra.

In general, the modeling of cloud drop spectra is relatively straightforward, since clouds usually are fairly stable for the purposes of droplet counting and sizing by modern instrumentation. The phenomenon of rain, on the other hand, represents highly unstable conditions so that it is difficult to define a generalized concept of raindrop density function without specifying several pertinent variables and meteorological conditions for each case. The easily recorded rainfall rate, R, is an integral over most such variables, and its dependence on droplet growth and breakup, fall velocities and updrafts, distance below cloud, etc., is not well known. Nevertheless, any extinction of electromagnetic flux by rain must be interpreted in terms of the "instantaneous" (really some sort of time and space average) drop-size distribution encountered by the beam. In radar meteorology these questions are usually bypassed by the adoption of empirical relations that seem to work in operational situations [Battan, 1973].

We shall introduce two raindrop density functions of the type (8) to simulate certain moderate and heavy rainfall conditions as suggested by careful consideration of recent drop-size measurements and simultaneous rainfall gauging. Our moderate rainfall model, called *rain-10*, is designed to represent drop-size distributions just below the cloud base when a precipitation rate of 10 mm hr^{-1} is measured at the ground. This model conforms to a distribution function

$$n(r) = a\, r^4\, e^{-12r}\ \text{m}^{-3}\ \text{mm}^{-1} \qquad (13)$$

where r_c = 1/3 mm and the constant a is fixed for a nominal N = 1000 drops per m^3. It will be noted that the model (13) distribution differs from the one we introduced earlier [Deirmendjian, 1969], called

rain L (for light rain aloft), notably in the choice of mode radius, for better agreement with Doppler radar data.

Our heavy rain model, called *rain-50*, is designed to represent raindrop spectra at ground level during rainfall rates of the order of 50 mm hr^{-1}. Its distribution function is given by

$$n(r) = a\, r^{6}\, e^{-10r}\ m^{-3}\ mm^{-1} \tag{14}$$

where r_c = 0.60 mm and a is fixed for N = 1000 drops per m^3.

The two models are illustrated by the solid continuous curves in Fig. 1, labeled "Rain-10" and "Rain-50." For comparison, one of the Doppler measurements obtained by Caton [1966] corresponding to a measured rate of 5.6 mm hr^{-1} and two of the ground-level measurements from Cataneo and Stout [1968] are also indicated on Fig. 1 by the labeled broken curves. Although the agreement is not perfect, our models are seen to be fairly representative of these particular measurements. This is sufficient for the purposes of the present report, designed to be an illustrative--but not comprehensive--study of the atmospheric attenuation to be expected for submillimeter waves.

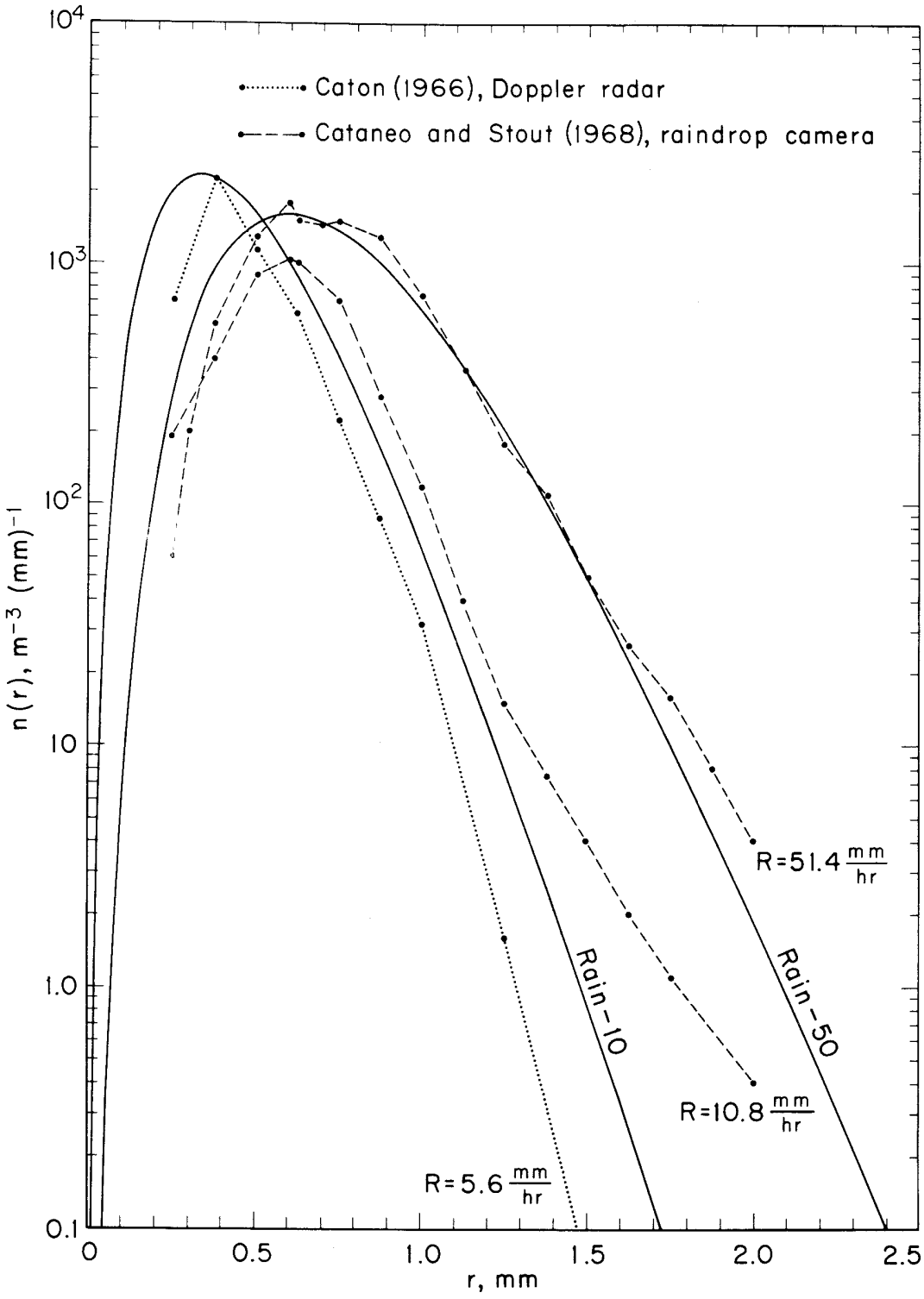

Fig. 1— Raindrop-size distribution models and some measurements

4. CHOICE OF WAVELENGTHS AND OPTICAL CONSTANTS

The optical constants for water in the far infrared were adapted from our own recent critical survey of available data presented as Part I of this report [Deirmendjian, 1974]. In Fig. 2 these are graphically reproduced again for easy reference. The various labeled curves are self-explanatory, and for the cited sources the reader is referred to Part I. As for the choice and number of wavelengths, a very high resolution is not necessary, due to the expected smooth variation of polydisperse scattering attenuation with wavelength. Our computations were made with sufficient coverage to allow for graphical interpolation between points.

For convenience we show in Table 1 the actual wavelengths we used together with the corresponding complex index values. Note that in the middle infrared some of these have been slightly changed from the values used previously [Deirmendjian, 1969] to bring them in line with the more recent determinations. For millimeter wavelengths we used the Debye formula values as in a previous study [Deirmendjian, 1963] valid for

Table 1

WAVELENGTHS AND COMPLEX INDICES OF REFRACTION

λ	$m = \nu - \kappa i$	λ	$m = \nu - \kappa i$
12.μm	1.111 - 0.199i	500.μm	2.22 - 0.740i
17.μm	1.376 - 0.429i	700.μm	2.32 - 0.890i
28.μm	1.549 - 0.338i	1000.μm	2.50 - 1.09i
40.μm	1.519 - 0.385i		
60.μm	1.703 - 0.587i	2.mm	2.5604 - 0.8947i
100.μm	2.06 - 0.551i	5.mm	3.1918 - 1.7657i
140.μm	2.07 - 0.470i	10.mm	4.2214 - 2.5259i
200.μm	2.08 - 0.509i	20.mm	5.8368 - 3.0046i
337.μm	2.20 - 0.600i	33.mm	7.1755 - 2.8642i

0°C water. In the $28 \lesssim \lambda \lesssim 1000$ μm spectral region, the optical constants shown are valid for room temperature or 24°C, as obtained by experiment, even though cloud- and raindrops are certainly at a lower temperature. Since the temperature dependence of the constants is uncertain at present [Deirmendjian, 1974] we prefer to use the original published values without modification.

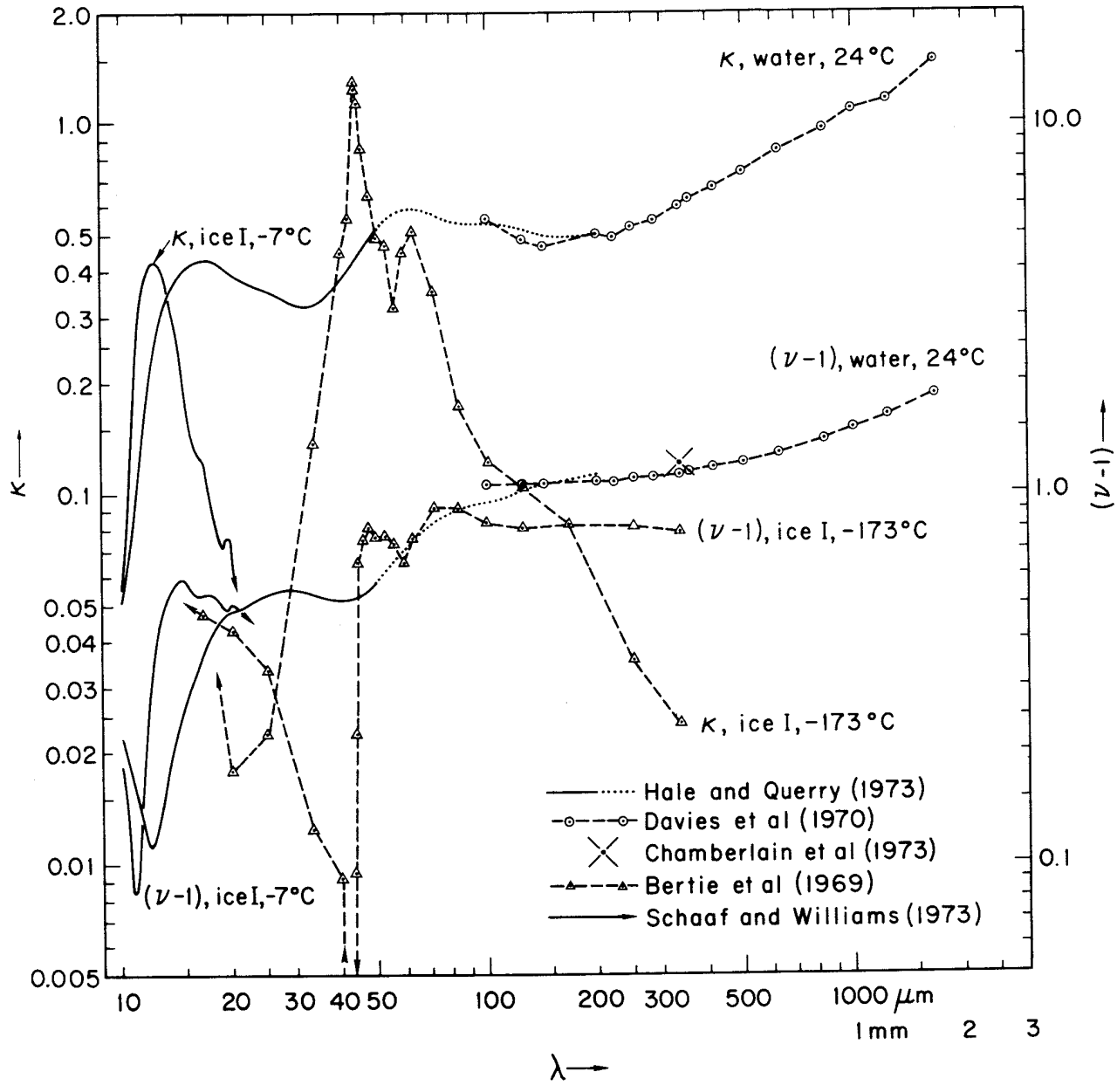

Fig. 2—Optical constants of water according to recent measurements

5. EXTINCTION COEFFICIENTS FOR CLOUDS AND RAIN

The polydisperse extinction coefficients were computed for the models described in Sec. 3 at the wavelengths and optical constants of Table 1 by the numerical techniques described previously [Deirmendjian, 1969]. Most of the computations were carried out in the IBM 370/158 system currently in use at Rand. Certain computational instabilities, arising for Bessel functions of complex argument whenever $\kappa x > 30$, were overcome without difficulty by using double precision arithmetic and forward recursion techniques as in previous instances [Deirmendjian, 1969].

Selected values of β_{ex} and the *volume absorption coefficient* β_{ab} (obtained by an integral similar to (2)) are listed in Tables 2 and 3. The difference, $\beta_{ex} - \beta_{ab} = \beta_{sc}$, is the *volume scattering coefficient*, as defined in radiative transfer formulations. The conventional units of (neper)* km^{-1} shown should really be interpreted as a cross-sectional area per unit volume, or in this case as $cm^2(10^5 cm^3)^{-1}$, such that the attenuated flux F of a plane-parallel or collimated stream of electromagnetic energy is given by

$$F = F_o \exp\{-\beta_{ex} L\} \tag{15}$$

where F_o is the source energy and L is the path length in kilometers through a homogeneous scattering medium. In Tables 2 and 3 the numbers shown in parentheses were obtained by approximations (3) and (6), as the case may be. The integrals (3) and (7) involved in these approximations may be easily evaluated from their analytic expressions in terms of gamma functions, after substituting the explicit forms for n(r) in each case and integrating between the limits r = 0 and ∞. For example the integral (3) takes the form

$$\beta_{ex}[n(r)] = 2\pi a \int_0^\infty r^{\alpha+2} e^{-br} dr$$

$$= 2\pi a\, \Gamma(\alpha+3)\, b^{-(\alpha+3)} . \tag{16}$$

*As used here and elsewhere in this report, the term "neper" refers to units of the exponential attenuation of power or energy flux, rather than of amplitude or voltage as in acoustical and electrical engineering usage.

Table 2

CLOUD VOLUME EXTINCTION AND ABSORPTION COEFFICIENTS
(Neper km^{-1})

	Cloud C.1 ($N = 10^2 cm^{-3}$)		Cloud C.5 ($N = 10^2 cm^{-3}$)		Cloud C.6 ($N = 10^{-1} cm^{-3}$)	
λ	β_{ex}	β_{ab}	β_{ex}	β_{ab}	β_{ex}	β_{ab}
($\lambda \to 0$)	(15.64)		(42.41)		(0.7540)	
12. μm	10.28	7.352	36.32	22.61	0.7933	0.4030
17. μm	16.12	10.23	49.98*	28.49*	0.8500*	0.4113*
28. μm	12.33	7.849	49.88	27.36	0.9004	0.4521
40. μm	8.468	6.392	39.86	24.89	0.9250	0.4774
60. μm	7.013	5.816	37.69	25.41	0.9742	0.5065
100. μm	2.690	2.415	20.70	14.55	1.061	0.553
140. μm	1.420	1.352	9.742	7.797	1.074	0.555
200. μm	0.9732	0.9570	5.617	5.109	0.9774	0.5190
337. μm	0.5812	0.5789	2.949	2.880	0.6845	0.4016
500. μm	0.4566	0.4560	2.235	2.219	0.4186	0.2911
700. μm	0.3474	0.3472	1.676	1.671	0.2563	0.2031
1000. μm		(0.2423)	1.165	1.164	0.1440	0.1274
2. mm		(0.0999)		(0.474)		(0.0401)
5. mm		(0.0381)		(0.181)		(0.0153)
10. mm		(0.0119)		(0.0563)		(0.0048)

*Values from an earlier run with m = 1.369 - 0.438i.

Table 3

RAIN VOLUME EXTINCTION AND ABSORPTION COEFFICIENTS
(Neper km^{-1}, $N = 10^3 m^{-3}$)

	Rain-10		Rain-50	
λ	β_{ex}	β_{ab}	β_{ex}	β_{ab}
($\lambda \to 0$)	(1.310)		(3.519)	
60.μm	1.396)	0.598		
100.μm	1.434	0.607	3.770	1.566
140.μm	1.462	0.635		
200.μm	1.502	0.666	3.905	1.677
337.μm	1.577	0.715	4.062	1.766
500.μm	1.651	0.769	4.218	1.868
700.μm	1.726	0.816	4.383	1.957
1000.μm	1.823	0.922	4.555	2.188
2.mm	1.950	1.017	5.043	2.518
5.mm	1.273	0.753	5.015	2.548
10.mm	0.3391	0.2640	2.293	1.452
20.mm	0.0675	0.0632	0.5101	0.4470
33.mm	0.0193	0.0188	0.1482	0.1408

For the limits $x_1(\lambda,r_1)$ and $x_2(\lambda,r_2)$ of the integral (2) we used the criterion that $n(r_1)$ and $n(r_2)$ should be less than $10^{-3}n(r_c)$, where $n(r_c)$ is the maximum of the density function. The upper limit in this case also conforms to the condition $r_2 > 2(\alpha+4)/b$, that is twice the value beyond which rapid convergence is assured according to condition (10). The integration steps were varied for each case to assure good accuracy without wasting machine time. Thus we believe that the values shown in Tables 2 and 3 are accurate to the four figures indicated and sufficient for present purposes.

The extinction coefficients in Tables 2 and 3 are also shown graphically in Fig. 3 where they are plotted as solid dots logarithmically against the wavelength. This is marked in micrometers and millimeters on the lower scale and the corresponding frequency in GHz is indicated on the top scale. The ordinate scale on the left shows the extinction coefficient in nepers per kilometer and on the right-hand scale in decibels per kilometer for convenience (conversion factor nepers to decibels: 4.343). The full curves are fitted "by eye" to the data points, and their dashed extensions connect the small particle approximations shown in parentheses in Tables 2 and 3. The dashed straight lines with arrows pointing to the left are the asymptotic values for large spheres according to (3).

For completeness and comparison we also extended the extinction evaluations of our original fair weather cumulus or cloud C.1 model [Deirmendjian, 1962, 1969] to the far infrared with the use of the new optical constants shown in Table 1. This model has a mode radius r_c of 4 μm and a water content of 0.063 g m^{-3} for a drop density of 100 cm^{-3}. The cloud C.1 far infrared and submillimeter extinction curve is included in Fig. 3 and the corresponding values are also listed in Table 2, including those at λ12 and 17 μm [Deirmendjian, 1969, Table T.49]. Note that the asymptotic value of 15.64 shown here is not quite reached by the λ0.45 μm extinction coefficient of 16.33 km^{-1}, obtained in the earlier work.

Tables 2 and 3 list the volume extinction and absorption coefficients for normalized *number* densities corresponding to the various models and may be used to scale these coefficients to other number

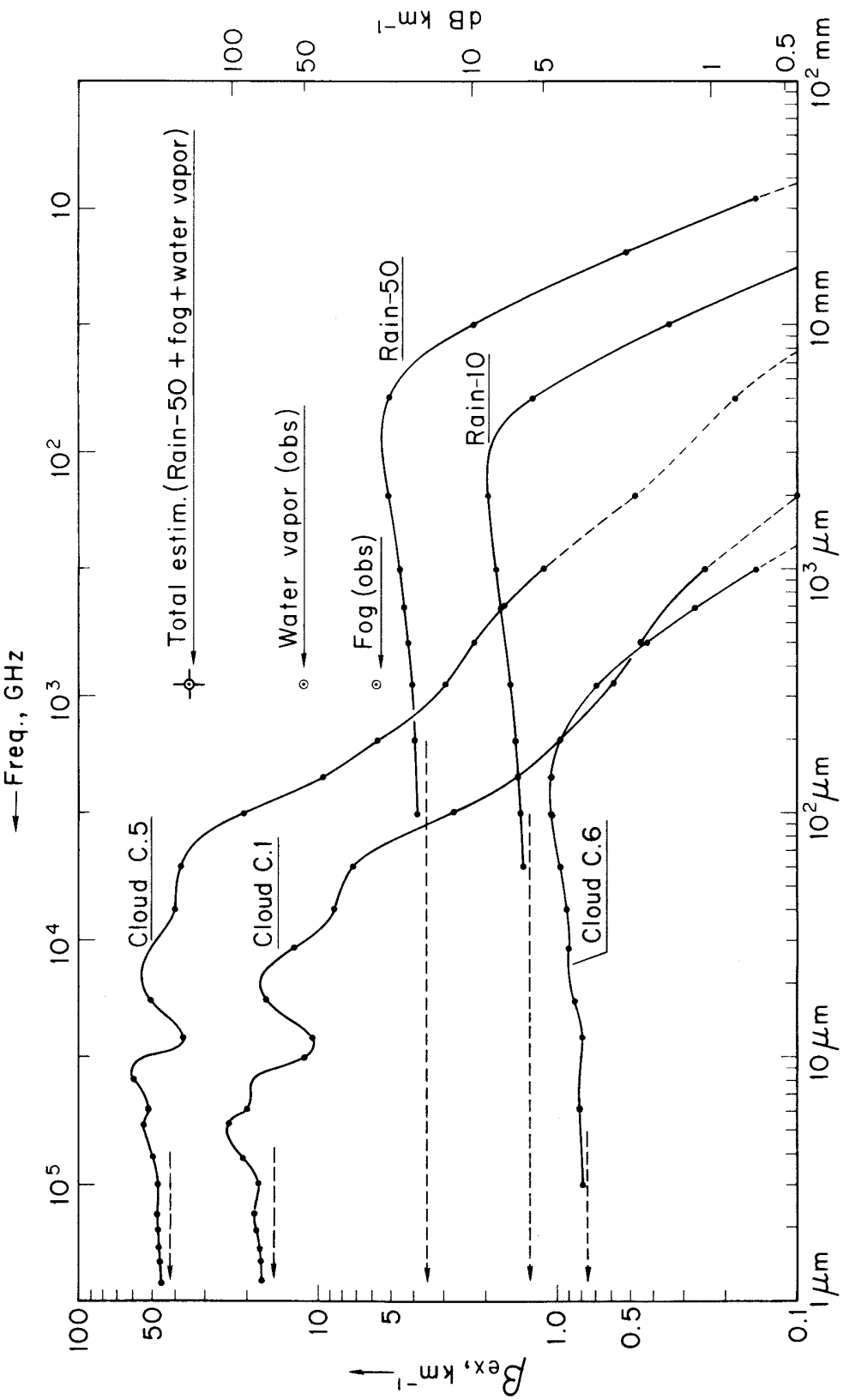

Fig. 3--Theoretical extinction coefficients according to three cloud models and two precipitation models

densities as given by observation or theoretical models approximating those adopted here. It is convenient and instructive to also consider the extinction coefficient per unit *mass* of particles. This may be obtained from the tables, provided the number of particles N_m per unit volume, per unit mass of substance, is known. The latter is given by the volume mixing ratio V_p as in (7) and the integrated number density N as in (9), that is

$$N_m = \frac{N}{\rho V_p} \tag{17}$$

where ρ is the density of the particle substance. In the case of water clouds and hazes, the *liquid water content* $w = \rho V_p$, usually expressed in grams per cubic meter, may be obtained from (17) by expressing V_p in cm^3 per m^3 with $\rho = 1$, or by setting $w = 10^6 V_p$. Consequently $10^{-6} N_m$ represents the number of particles per unit volume per g m^{-3} of liquid water content. The mass extinction coefficient γ_{ex} is therefore obtained from β_{ex} by writing

$$\gamma_{ex}[n(r),w] = 10^{-6} \frac{N_m}{N} \beta_{ex} = w^{-1} \beta_{ex} \quad . \tag{18}$$

In Table 4 we list sample values of the mass extinction coefficients for two of our cloud models C.1 and C.5, the rain model rain-10, and for comparison our haze model haze L (r_c = 0.07 μm) corresponding to a continental type distribution [Deirmendjian, 1969]. The use of parentheses in Table 4 has the same meaning as in Tables 2 and 3. The reader can derive other values by use of equation (18) and the liquid water contents shown under each model in Table 4. These values may be used to scale the extinction of clouds and rain for liquid water contents other than those adopted in our models, *provided that the size distribution can be approximated by these models.* In fact, as is clear from Table 4, for a given water content the amount of extinction produced by water particles depends very much on their relative size and number distribution. The mass extinction coefficient at any given wavelength becomes constant only when all the particles in the distribution

Table 4

MASS EXTINCTION COEFFICIENTS FOR HAZE, CLOUDS, AND RAIN
(γ_{ex} in neper km^{-1} per g m^{-3} liquid water content)

λ	Haze L $w = 1.167 \cdot 10^{-5}$ g m^{-3}	Cloud C.1 $w = 0.06255$ g m^{-3}	Cloud C.5 $w = 0.2969$ g m^{-3}	Rain-10 $w = 0.5091$ g m^{-3}
($\lambda \to 0$)	(3117.)	(250.1)	(142.8)	(2.573)
16.6μm	247.6			
17.0μm		257.8	168.3	
100.μm	(36.8)	43.01	69.72	2.816
200.μm	(16.8)	15.56	18.92	2.950
337.μm	(10.5)	9.293	9.932	3.097
500.μm	(7.21)	7.301	7.527	3.243
1.mm	(3.87)	(3.87)	3.924	3.580
2.mm	(1.60)	(1.60)	(1.60)	3.830

are small compared to the wavelength. This is demonstrated by the λ1 and 2 mm values in the table, which are independent of the model except in the rain-10 case where the drop diameters are of the order of the wavelength.

6. DISCUSSION AND CONCLUSIONS

As may be seen from Tables 2 and 3 and Fig. 3, the highest water droplet extinctions are to be expected from stratus cloud or fog (cloud C.5) at $\lambda \lesssim 200$ μm. Here the computed extinction coefficients, reaching a magnitude of 50 nepers or over 200 decibels per kilometer, may even be underestimated by factors of two or three considering that real clouds may contain 200 to 300 droplets per cm^3. However, beyond $\lambda 100$ μm the cloud extinction falls more-or-less as λ^{-1}, reaching values below those for moderate rain beyond $\lambda 1$ mm.

A comparison of the extinction curves for the fair weather cumulus C.1 and stratus cloud C.5 shows them to be approximately parallel, both showing the relative "window" in the $10 \lesssim \lambda \lesssim 12$ μm region. At shorter wavelengths toward the visible the extinction ratio $\beta_{ex}(C.1)/\beta_{ex}(C.5)$ is given by that of the asymptotic values for $\lambda \to 0$ listed in Table 2, that is, 0.37, which is also the ratio of the corresponding integrated geometric cross sections (3). At wavelengths longer than $\lambda 1$ mm the same ratio is seen to be 0.21, which is exactly that of the water contents of the two models, as follows from the discussion of the small particle approximation (6). The contribution of cloud C.6, as expected, is seen to be quite small compared to those of the other models except in the region $\lambda > 100$ μm where it is of the same order as the cloud C.1 extinction.

In the real world, of course, the extinction by clouds may vary considerably--though not by an order of magnitude--from the estimates given here, depending on the cloud type, water content, form, homogeneity, etc. Our estimates are for illustrative purposes only and do not include, for example, the very important contribution by the strong water vapor absorption bands known to exist in the entire region. This subject is not within the scope of the present report, but we note the H_2O absorption may exceed the cloud extinction according to theoretical estimates [Birch et al, 1969].

The rain extinction curves are quite smooth and approach their asymptotic values quickly for wavelengths shorter than 100 μm or so.

(These asymptotic values, of course, are very good estimates of the attenuation of visible radiation by rain. Compare for example our value of 1.31 km^{-1} for rain-10 with that of 1.32 km^{-1} obtained independently by Chen [1974] for "medium rain" of 12.5 mm hr^{-1} intensity.) At the other end of the spectrum, note from the last line in Table 3 that at λ3.3 cm the ratio 7.68 of the extinction for the rain-50 and rain-10 models differs significantly from that of their respective water contents, namely 2.11/0.509 = 4.15. This demonstrates that the small sphere approximation (6) is not good enough at this wavelength, as pointed out in an earlier study [Deirmendjian, 1963]. From Fig. 3 and Table 3 a maximum value in rain extinction occurs somewhere between λ2 and λ5 mm for both models, in a region where the cloud effect is small and dropping rapidly toward longer waves.

A rough comparison of our rain extinction estimates with independent evaluations is possible only at millimeter wavelengths and may be obtained by graphical interpolation on data adapted from the literature by Dudzinsky [1974]. For a rainfall rate of 50 mm hr^{-1}, our value and that estimated by D. E. Setzer [Dudzinsky, 1974, Fig. 1] coincide exactly at λ10 mm, while at λ33 mm our value is somewhat lower than Setzer's estimate. Similarly, our rain-50 model values fall between the "world" measured maximum and minimum attenuations as given by Medhurst and summarized by Dudzinsky [1974, Fig. 3]. These microwave data stop at about λ5 mm. For any shorter wavelengths there are few, if any, observations and our predicted values here may be useful in the design of future experimental programs.

For the cloud extinction values in the submillimeter region there are few independent determinations and fewer experimental values to allow a comparison. A good determination, on the basis of a series expansion of K_{ex}, is provided by Platt [1970]. Platt used the second and third terms [cf. Deirmendjian, 1963, App. B], in addition to the first as in equation (4), to obtain the contribution from the larger droplets at λ200 and λ337 μm, his two shortest wavelengths, and the best optical constants available at the time of his work. We compare below his determinations for a typical fog distribution with our own model values as in Table 4, after converting Platt's values to the same units of nepers per kilometer per unit liquid water content:

	λ 200 μm	λ 337 μm
Platt [1970], fog	21.4	9.46
Cloud C.1 (N_m = 1599)	15.6	9.29
Cloud C.5 (N_m = 337)	18.9	9.93

Considering the differences in method and drop-size distribution, the agreement is quite good, especially at the longer wavelength as expected, and corroborates Platt's [1970] approximation.

Finally a comparison with available measurements of attenuation in the natural atmosphere is useful as a check of the validity of our models. Unfortunately there appears to be a lack of measurements over a wide enough portion of the far infrared spectrum to allow a good comparison. The point marked "Fog (obs)" on Fig. 3 is adapted from one of the few published atmospheric determinations at the HCN laser wavelength of λ337 μm [Burroughs et al, 1966] obtained in fog with a visibility of 35 m. Now the Koschmieder empirical formula, modified according to Middleton's [1952] discussion by R. E. Huschke [personal communication] may be written

$$\beta_{ex} = \frac{3.352}{\text{visibility}} \tag{19}$$

which yields an extinction coefficient of about 96 nepers per kilometer at visible wavelengths during the HCN laser observation. From Table 2 we note that this is about double the short wave asymptotic value for our cloud C.5 model, which comes closest to a fog-type droplet distribution. Hence we may assume that the fog contained about 200 droplets per cm^3 or a liquid water content of about 0.6 g m^{-3}, not at all unreasonable numbers according to previous measurements [Mason, 1971]. The equivalent extinction coefficient at λ337 μm from Table 2 is 5.9 km^{-1} which checks very well with the Burroughs et al [1966] measurement of 25 dB or 5.8 neper per kilometer.

The point on Fig. 3 marked "water vapor (obs)" is also adapted from the same source [Burroughs et al, 1966], which cites an absolute humidity of 4.84 g m^{-3} observed during the experiment. The water vapor

absorption of 11.5 km^{-1}, measured over a horizontal path, indicates the magnitude of this component in the absence of clouds. Within precipitating clouds under saturation conditions, the absolute humidity may be of the order of 10 g m^{-3} with a corresponding increase in water vapor absorption.

To get an idea of the magnitude of attenuation to be expected under conditions of fog and heavy rain in the path of a beam of $\lambda 337$ μm radiation, the crossed circle on Fig. 3, marked "total estim.," shows an estimate arrived at as follows:

	Nepers km^{-1}	Decibels km^{-1}
H_2O absorption (10 g m^{-3})	24.0	104.
Cloud C.5 (w = 0.6 g m^{-3})	5.90	25.6
Cloud C.6	0.68	2.95
Rain-50	4.06	17.6
Total	34.64	150.2

Clearly, elimination of the rain attenuation in this case would make a difference of only about 10 percent, the heaviest contribution being that of water vapor absorption bands. Other examples of attenuation may be obtained by applying the pertinent models to hypothetical situations with various amounts of water vapor and types and extent of cloud and rain encountered along a given path.

As to attenuation by other types of cloud and precipitation composed of ice particles, snow, and hail, an accurate theoretical estimate is unobtainable at present, since (a) the effects of the irregularity of their shape are not well known except for highly idealized models, and (b) the optical constants for ice in the submillimeter region are so far available only for unrealistically low temperatures [Deirmendjian, 1974]. However, a rough idea of their attenuating properties could be obtained in certain areas by using the asymptotic approximations discussed earlier, if the number density and size distribution of ice particles are known.

For possible future millimeter communication systems within the atmosphere, the scope of the present study is sufficient to provide a

good estimate of the attenuating effects of clouds and rain up to a wavelength of $\lambda 20$ mm. These of course apply only to power degradation but not to phase and coherence losses caused by coherent scattering and turbulence effects. Water vapor absorption under atmospheric conditions also needs further study before choosing likely window regions for millimeter and submillimeter wave propagation. There seem to be several window-like bands in the region $0.83 \lesssim \lambda \lesssim 8.6$ mm, according to work discussed in two recent symposia [Fox, 1971; Button, 1974], but usually these are the result of theoretical estimates or laboratory determinations. On their basis and in the light of our present results it would seem that, in the presence of nonprecipitating water clouds, the relative "window" around $\lambda 1.3$ mm or a frequency of 230 GHz might be a good compromise. At this frequency Wrixon [1974] has obtained a fairly good estimate of the "clear sky" zenith attenuation, of about 1 dB, by using the reliable Bouguer-Langley method and solar millimeter radiation. As may be seen from Fig. 3, this attenuation is of the same magnitude as that through 1 km of cloud C.1. Precipitating type clouds, fog, or rain, however, would increase the attenuation by at least a factor of five.

The extinction coefficients for clouds and rain for any window region in the near millimeter spectrum may be easily estimated with good accuracy from our results, for example by graphical interpolation on plots of our tabulated values as in Fig. 3.

REFERENCES

Battan, Louis J. (1973). *Radar Observation of the Atmosphere.* University of Chicago Press, Chicago, 324 pp.

Birch, J. R., W. J. Burrows, and R. J. Emery (1969). Observation of atmospheric absorption using submillimetre maser sources. *Infrared Physics*, 9, 75-83.

Burroughs, W. J., E. C. Pyatt, and H. A. Gebbie (1966). Transmission of sub-millimetre waves in fog. *Nature*, 212 (5060), 387-388.

Button, Kenneth J. (ed.) (1974). Proceedings First International Conference on Submillimeter Waves and their Applications. *IEEE Trans. Microwave Theory Tech.*, MTT-22 (12 Part I), 981-1120.

Cataneo, R., and Glenn E. Stout (1968). Raindrop-size distributions in humid continental climates, and associated rainfall rate-radar reflectivity relationships. *J. Appl. Meteor.*, 7 (5), 901-907.

Caton, P.G.F. (1966). A study of raindrop-size distributions in the free atmosphere. *Quart. J. R. Met. Soc.*, 92 (391), 15-30.

Chen, C. C. (1974). *A Correction for Middleton's Visible- and Infrared Radiation Extinction Coefficients Due to Rain.* R-1523-PR, The Rand Corporation, Santa Monica, California, 10 pp.

Chýlek, Petr (1973). Large-sphere limits of Mie-scattering functions. *J. Opt. Soc. Amer.*, 63 (6), 699-706.

Deirmendjian, D. (1962). *Scattering and Polarization Properties of Polydispersed Suspensions with Partial Absorption.* RM-3228-PR, The Rand Corporation, Santa Monica, California, 34 pp.

Deirmendjian, D. (1963). *Complete Microwave Scattering and Extinction Properties of Polydispersed Cloud and Rain Elements.* R-422-PR, The Rand Corporation, Santa Monica, California, 54 pp.

Deirmendjian, D. (1964). Scattering and polarization properties of water clouds and hazes. *Appl. Optics*, 3 (2), 187-196.

Deirmendjian, D. (1969). *Electromagnetic Scattering on Spherical Polydispersions.* American Elsevier, New York, 290 pp.; also *Electromagnetic Scattering on Spherical Polydispersions.* R-456-PR, The Rand Corporation, Santa Monica, California.

Deirmendjian, D. (1974). *Far Infrared and Submillimeter Scattering I. The Optical Constants of Water--A Survey.* R-1486-PR, The Rand Corporation, Santa Monica, California, 19 pp.

Dudzinsky, S. J., Jr. (1974). *Atmospheric Effects on Terrestrial Millimeter-Wave Communications.* R-1335-ARPA, The Rand Corporation, Santa Monica, California, 37 pp.

Fox, Jerome (ed.) (1971). *Proceedings of the Symposium on Submillimeter Waves.* Polytechnic Press, New York, 726 pp.

Hansen, J. E. (1971). Multiple scattering of polarized light in planetary atmospheres. Part II. Sunlight reflected by terrestrial water clouds. *J. Atmos. Sci.*, 28 (8), 1400-1426.

Hulst, H. C. van de (1957). *Light Scattering by Small Particles.* J. Wiley & Sons, New York, 450 pp.

Kattawar, George W., and Gilbert N. Plass (1975). Interior radiances in optically deep absorbing media-III. Scattering from haze L. *J. Quant. Spectrosc. Radiat. Transfer*, 15, 61-85.

Mason, B. J. (1971). *Cloud Physics* (2nd ed.). Clarendon Press, Oxford, 671 pp.

Middleton, W.E.K. (1952). *Vision through the Atmosphere.* University of Toronto Press, Toronto, 250 pp.

Okita, T. (1961). Size distribution of large droplets in precipitating clouds. *Tellus*, 13 (4), 509-521.

Penndorf, Rudolf B. (1962). Scattering and extinction coefficients for small absorbing and nonabsorbing aerosols. *J. Opt. Soc. Amer.*, 52 (8), 896-904.

Platt, C.M.R. (1970). Transmission of submillimeter waves through water clouds and fogs. *J. Atmos. Sci.*, 27 (3), 421-425.

Thompson, B. C., and M. B. Wells (1971). Scattered and reflected light intensities above the atmosphere. *Appl. Opt.*, 10 (7), 1539-1549.

Wrixon, G. T. (1974). Measurements of atmospheric attenuation on an earth space path at 230 GHz using a sun tracker. In *Proc. 4th European Microwave Conference*, F. Gardiol (ed.), Microwave Exhibitions and Publishers Ltd., England, 222-226.